



HAL
open science

Catalytic hydrotreatment of algal HTL bio-oil over phosphide, nitride, and sulfide catalysts

Bruno da Costa Magalhaes, Ruben Checa, Chantal Lorentz, Mathieu Prévot, Pavel Afanasiev, Dorothee Laurenti, Christophe Geantet

► **To cite this version:**

Bruno da Costa Magalhaes, Ruben Checa, Chantal Lorentz, Mathieu Prévot, Pavel Afanasiev, et al.. Catalytic hydrotreatment of algal HTL bio-oil over phosphide, nitride, and sulfide catalysts. ChemCatChem, 2023, 10.1002/cctc.202300025 . hal-04045206

HAL Id: hal-04045206

<https://hal.science/hal-04045206>

Submitted on 24 Nov 2023

HAL is a multi-disciplinary open access archive for the deposit and dissemination of scientific research documents, whether they are published or not. The documents may come from teaching and research institutions in France or abroad, or from public or private research centers.

L'archive ouverte pluridisciplinaire **HAL**, est destinée au dépôt et à la diffusion de documents scientifiques de niveau recherche, publiés ou non, émanant des établissements d'enseignement et de recherche français ou étrangers, des laboratoires publics ou privés.

Catalytic hydrotreatment of algal HTL bio-oil over phosphide, nitride, and sulfide catalysts

Bruno C. Magalhães,^[a] Ruben Checa,^[a] Chantal Lorentz,^[a] Mathieu Prévot,^[a] Pavel Afanasiev,^[a] Dorothée Laurenti,^[a] and Christophe Geantet^{*[a]}

[a] IRCELYON, UMR-CNRS 5256, Université Claude Bernard Lyon 1
2 av A. Einstein, F-69626 Villeurbanne Cedex (France)
E-mail: christophe.geantet@ircelyon.univ-lyon1.fr

Supporting information for this article is given via a link at the end of the document.

Abstract: Global energy demand and environmental concerns about limiting CO₂ emissions have been growing recently. This is why fuel production from renewable resources has become a priority. In this context, microalgae represent an attractive alternative carbon source. In this work, different supported catalysts, including metal phosphide, nitride, and sulfide, were tested for the hydroconversion of bio-oil issued from the hydrothermal liquefaction of microalgae. Supported Ni phosphide catalysts promoted the decarboxylation and decarbonylation route, while NiMo nitride promoted the hydrodeoxygenation pathway. NiW sulfide catalysts were the most performant, producing a hydrotreated oil with the best higher heating value (HHV), lower aromaticity degree, and lower average molar mass. Among sulfide catalysts, NiWS/SiO₂-Al₂O₃ was the least active, probably due to the inhibition of acid sites by the nitrogen compounds. However, NiWS/Al₂O₃ performed better, showing high hydrogenation performances, which contributed to the conversion of refractory compounds.

Introduction

Microalgae are potentially biomass sources for producing third-generation biofuels due to their ability to convert solar energy through photosynthesis, capture CO₂, and store this carbon in energy-rich compounds such as lipids.^[1,2] These microorganisms have high-speed growth rates, resulting in high productivity.^[3] Hydrothermal liquefaction (HTL) is a thermochemical process that allows the conversion of wet biomass such as microalgae, avoiding a costly drying step.^[4,5] The lipids are hydrolyzed, forming carboxylic acids that can be further converted into drop-in fuels for diesel and jet fuel.^[6] Besides, the carbohydrates and proteins can also be converted, affecting the quality and properties of the HTL bio-oil as a function of microalgae biochemical composition.^[7,8]

The algal HTL bio-oil has high oxygen (~5 – 20 wt.%) and nitrogen content (~2–9 wt.%), as well as sulfur (~0–1 wt.%) and metals.^[9–12] Therefore, an upgrade is required to convert the HTL bio-oil into drop-in fuels to be compatible with traditional engines.^[13] Catalytic hydrotreatment (HDT) is conducted at moderate temperatures (300 – 450 °C), under hydrogen pressure (35 – 170 bar), with a liquid hourly space-velocity of 0.2–10 h⁻¹, and in the presence of a heterogeneous catalyst.^[14]

Supported Mo or W sulfides are traditional hydrotreating catalysts, and some works have demonstrated their efficacy in upgrading algal HTL bio-oil.^[15–19] These nanomaterials are usually supported

on γ -alumina and are promoted by nickel or cobalt.^[20] Moreover, these catalysts can also be boosted by adding another element, such as phosphorus^[21,22] or a chelating agent (e.g., citric acid).^[23,24]

Biller *et al.*^[25] employed NiMo/Al₂O₃ and CoMo/Al₂O₃ sulfide catalysts to upgrade algal HTL bio-oils and reported that both catalysts showed similar activity during hydroprocessing. Later, Guo *et al.*^[26] compared commercial NiMo/Al₂O₃ and NiW/Al₂O₃ and concluded that NiMo performed better in removing oxygen and nitrogen. However, the highest sulfur removal was achieved by the NiW catalyst.

Moreover, other types of catalysts, such as metal phosphides, carbides, and nitrides, have been considered in the literature as promising for bio-oils upgrading.^[27,28]

Bowker *et al.*^[29] tested silica-supported Ni phosphide catalysts (Ni₂P) for the hydrodenitrogenation (HDN) of carbazole with and without a benzothiophene co-feed. They reported that phosphide catalysts exhibited excellent stability in the HDN reactions and performed better than NiMo/Al₂O₃ sulfide, even if benzothiophene inhibited the carbazole HDN over the metal phosphide catalysts. Besides, Cole *et al.*^[30] achieved 80% nitrogen conversion using Ni₂P/SiO₂ to upgrade a blended feed with 3230 N ppm composed of bio-oil from algae HTL and green hydrocarbons from the CO₂ hydrogenation.

Phosphide catalysts are usually prepared by the temperature-programmed reduction (TPR) of phosphate-based precursors in flowing hydrogen at high temperatures.^[31] This method can lead to large Ni₂P particles (> 10 nm), side reactions between surface P and aluminum in Al-containing support (e.g., γ -Al₂O₃ and ASA), and can also make difficult the *in situ* preparation of metal phosphide in the industrial hydrotreating reactors.^[32] In this context, d'Aquino *et al.*^[33] reported a preparation method of Ni phosphide over oxide supports from nickel hypophosphite precursors and their reduction at lower temperatures. Their results showed well-dispersed catalysts with small particles sizes (3–4 nm), which were highly active for an HDN and hydrodesulfurization (HDS) of a mixed carbazole (1000 ppm)/benzothiophene (3000 ppm) feed. Ni₂P/SiO₂ and Ni₂P/Al₂O₃ *in situ* prepared catalysts showed higher HDN and HDS conversion than commercial NiMo/Al₂O₃ sulfide.

Regarding metal nitride catalysts, Sajkowski and Oyama^[34] compared unsupported Mo nitride against commercial NiMo/Al₂O₃ sulfide for hydrotreating coal-derived gas oil and residues. They showed that Mo nitride was active under the experimental hydrotreating conditions. Besides, Chu *et al.*^[35] tested a series of NiMoN_x/Al₂O₃ catalysts with different Ni content

RESEARCH ARTICLE

prepared by the temperature-programmed reaction of NiO.MoO₃/Al₂O₃ with NH₃. Those nitride catalysts showed higher pyridine HDN activity than NiMo/Al₂O₃ sulfide, which was associated with the new phase of Ni₃Mo₃N and the synergy between metallic Ni and nitride Mo. Mo₂N phase and Ni metal were also found in the NiMoN/Al₂O₃ catalysts.^[36]

Moreover, Chouzier *et al.*^[37] reported a one-step way to prepare bimetallic nitrides Co(Ni)-Mo from the decomposition of transition metal complexes with hexamethylenetetramine (HMTA) under an inert atmosphere. Then, they studied binary and ternary nitrides prepared via this methodology in the hydrotreatment reaction.^[38] Thiophene hydrodesulfurization (HDS) and quinoline HDN tests showed that bimetallic nitrides were highly active HDN catalysts in the absence of sulfur, but no synergy effect was observed for thiophene HDS.

Overall, phosphide and nitride catalysts have shown promising results compared to conventional sulfide catalysts, which are highly employed in refineries. However, these investigations were mainly carried out with model molecules, whereas the applicability of phosphides and nitrides to real bio-oil charges remains to be clarified.

In order to achieve high yield and selectivity to the desired products, the catalyst plays an essential role during this process, and a careful catalyst screening for upgrading algal HTL bio-oils under hydrotreating (HDT) conditions still needs to be achieved. In this context, supported Ni phosphides, supported and unsupported Mo nitrides catalysts were synthesized and compared with various supported NiMo and NiW sulfide catalysts to upgrade algal bio-oil. The hydrotreated oils were characterized by several analytical techniques to follow the reaction and understand the catalyst impact during the HDT stage.

Results and Discussion

Transmission electron microscopy (TEM) images of metal phosphides, nitrides, and sulfides are reported in the supplementary material, Figure S1. The Ni phosphide catalyst supported on silica showed nanoparticles of Ni₂P well dispersed, which was also corroborated by the XRD pattern (See Figure S2). However, the Ni phosphide catalyst supported on alumina showed large particles, which disagrees with the results reported by d'Aquino *et al.*^[33] (3.9 nm ± 0.6). Besides, the XRD pattern for this catalyst evidenced the formation of the Ni₂P phase. Ni₅P₄ impurities was also found. For the unsupported and supported NiMo catalyst, the TEM images reveal isotropic nanoparticles, and the XRD pattern of the NiMo nitride catalyst over alumina confirmed the formation of the Ni₂Mo₃N phase. The NiW sulfide catalyst, prepared with and without citric acid, showed 3-5 nm WS₂ slabs with homogenous distribution of the Ni promoter over the W sulfide (see Figure S1 and Table S1).

The HTL algal oil, provided by our partner, was analyzed. The main components in this oil are the C16 and C18 fatty acids (34 wt.%) coming from the hydrolysis of the triglycerides during the HTL process. The yield of oils and solids after HDT over the different catalysts were around 50-70 wt.% and 6-12 wt.%, respectively. The gases were not quantified but missing masses can be attributed to gas mainly in addition to experimental losses and water (Table S2).

The elemental analysis of the HTL and HDT oils with and without catalysts are reported in Table 1. A commercial green diesel composed mainly of C15-C18 aliphatics obtained from the hydroconversion of palm oil was used as a reference for comparison with HDT algal oil.

The oxygen content of the HTL oil was highly reduced in the HDT step, even without a catalyst. The high oxygen content in HTL oil is due to the fatty acids, rapidly converted under the HDT experiment conditions by hydrogenolysis reactions or by decarboxylation which can occur without a catalyst.^[39,40] However, only 20% denitrogenation degree was achieved without a catalyst, indicating that these molecules are more difficult to be converted by a thermal process. The Ni phosphide catalysts promoted both HDO and HDN reactions. However, differently to that reported by d'Aquino *et al.*,^[33] the *ex situ* Ni₂P/Al₂O₃ prepared from hypophosphite precursor was more active than Ni₂P/SiO₂ prepared from phosphate-based precursors.

The NiMo nitride catalyst supported over alumina showed an HDN activity (65%) significantly higher than the bulk NiMo nitride catalyst (46%), indicating that the alumina support could promote this reaction by dispersing the active phase.

Among the sulfide catalysts tested, NiWS/Al₂O₃ was the most active, resulting in an HDT oil with lower heteroatom content and greater HHV. No benefit effect was found after a post-treatment of the nickel tungsten catalyst with citric acid (NiWS/Al₂O₃ + CA) since the results were very similar to those found for the NiWS/Al₂O₃ without a chelating agent (see Table S3). Besides, the catalyst prepared by the co-impregnation methodology (NiW(CA)S/Al₂O₃) was tested in a feed with thiophene as the model molecule and showed approximately 30% higher thiophene HDS activity than the NiWS/Al₂O₃, as reported in Figure S3. However, this catalyst showed poor HDN activity for upgrading algal bio-oil, resulting in an HDT oil with two times more nitrogen compared to the results obtained with NiWS/Al₂O₃. The NiWS/SiO₂-Al₂O₃ catalyst also showed poor HDN activity compared to the NiWS/Al₂O₃, even though the metal loadings were very similar. This activity trend can be attributed to the inhibition provoked by the strong adsorption of nitrogen compounds, mainly basic compounds in the algal HTL bio-oil.^[41,42] Lastly, the NiMo(P)S/Al₂O₃ showed close results to the NiWS/Al₂O₃ catalyst, which performed slightly better.

Van Krevelen's diagrams given for O/C and N/C versus H/C (Figure 1) showed a significant improvement in the heteroatom reduction when a catalyst was employed, alumina supported NiWS catalyst being the closest but still far to the green diesel. More severe reaction conditions or the utilization of a second upgrading stage must be used to produce diesel-like oil.^[43]

To provide a deeper understating of the HDT over different active phases, other analytical techniques were used to characterize the HDT oil obtained over Ni₂P/Al₂O₃, NiMoN/Al₂O₃, and NiWS/Al₂O₃.

Table 1. Elemental analysis of HTL and HTD-oils.

Sample	C	H	O	N	S	HHV
HTL bio-oil	72.2	9.8	11.7	2.6	2125*	35.5
Without cat.	82.8	13.0	1.5	2.1	259*	44.1

RESEARCH ARTICLE

Ni ₂ P/Al ₂ O ₃	84.0	13.2	0.8	1.0	134*	44.7
Ni ₂ P/SiO ₂	84.5	13.2	1.0	1.6	273*	44.9
NiMoN	85.0	13.6	0.9	1.4	243*	45.6
NiMoN/Al ₂ O ₃	84.0	13.6	1.0	0.9	198*	45.2
NiWS/Al ₂ O ₃	84.8	14.2	0.7	0.6	57*	46.3
NiWS/SiO ₂ -Al ₂ O ₃	84.3	13.6	0.9	1.2	236*	45.3
NiMo(P)S/Al ₂ O ₃	84.7	13.6	0.8	0.8	101*	45.5
Green diesel	84.7	15.7	0.0	0.0	0.0	48.1

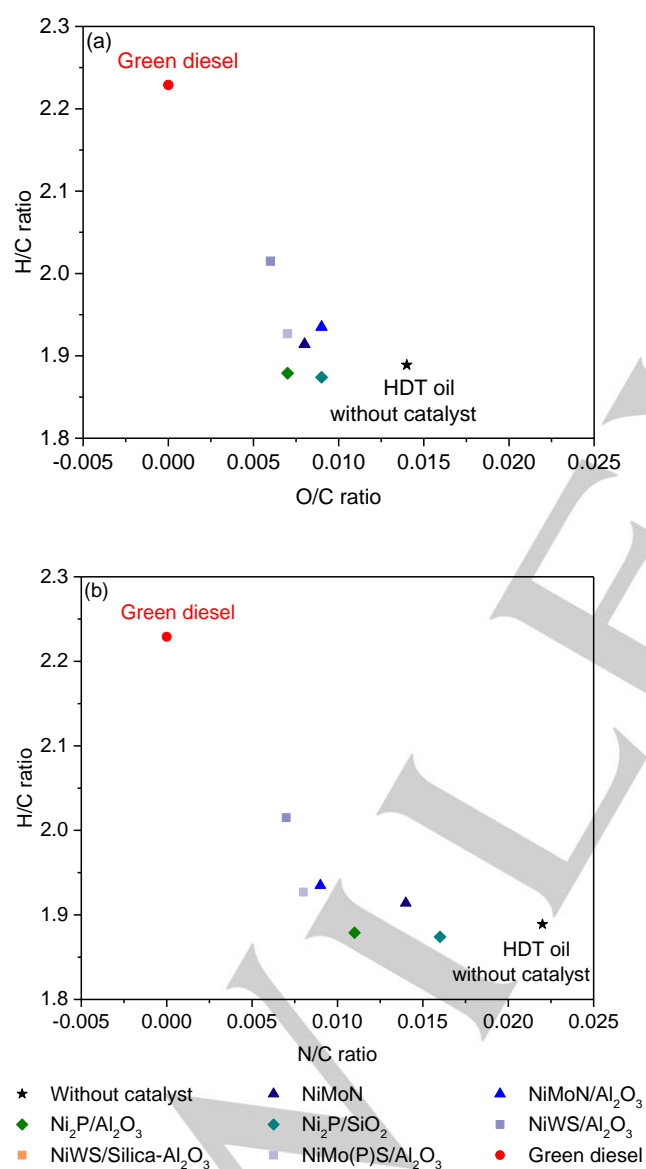
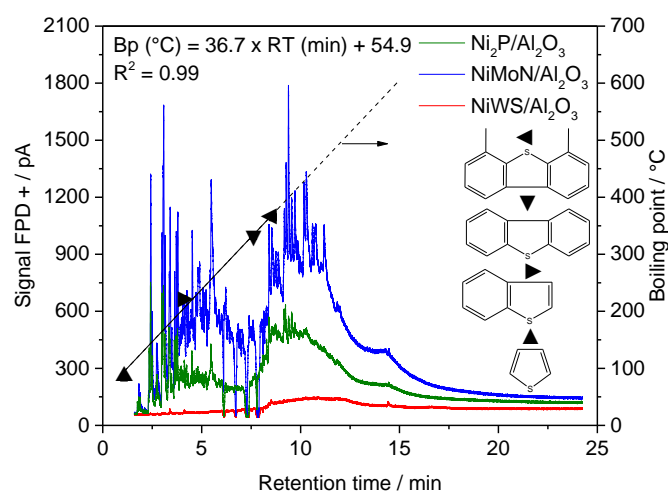


Figure 1. Van Krevelen's diagrams of upgraded HTL bio-oil with and without catalyst: (a) O/C and (b) N/C. A commercial green diesel from palm oil, composed mainly of aliphatics, was used as a reference.

The sulfur content in the algal HTL oil is relatively low compared to other oils.^[44] These molecules are derived primarily from amino acids which contain sulfur, such as cysteine and methionine, and sulfate lipids. The structures of the sulfur molecules that can be present in those oils and their reactivity are rarely reported in the literature.^[45] In order to go further in this S analysis, a gas chromatography (GC) coupled with a flame photometric detector plus (FPD+), highly selective for sulfur and phosphorous components, was employed to analyze the samples of oil hydro-treated over different catalysts. Thiophene, benzothiophene, dibenzothiophene, and 4,6-dimethylidibenzothiophene (4,6-DMDBT) were used as standards, and their retention time in function of the boiling point was plotted, as shown in Figure 2.

A high linear correlation ($R^2 > 0.99$) was found between the retention time and the boiling point of the sulfur standards. An extrapolation of this curve was employed to provide insights regarding the sulfur species in HDT oil. As demonstrated by the elemental analysis, the sulfur content in the HDT oil treated over NiMoN/Al₂O₃ was higher than those obtained with NiWS/Al₂O₃ and Ni₂P/Al₂O₃, resulting in a more intense FPD+ signal with the first catalyst. Besides, four negative peaks can be observed around 5- and 10-min. These peaks can be attributed to the C15, C16, C17, and C18 n-alkanes, present in high amounts in the HDT oil, as will be discussed further. Several peaks with retention time close to benzothiophene were found (2-7 min). These peaks can be associated with light sulfur compounds and were highly reduced in the function of the sulfur content in the HDT oil.

Thin and broad peaks with retention time fitting with dibenzothiophene and higher than the 4,6-DMDBT were also found (7-15 min) and can be associated with heavy sulfur compounds. The peak's shapes indicate that the heavy sulfur compounds are distributed into several molecules, which can justify why these compounds are so difficult to be characterized. Moreover, the Ni₂P/Al₂O₃ resulted in an HDT oil with lower sulfur content compared to the NiMoN/Al₂O₃, showing a significant reduction of light and heavy sulfur compounds. Lastly, the NiWS/Al₂O₃ exhibited the highest hydrodesulfurization activity. The residual sulfur present in this HDT oil can be associated mainly with heavy sulfur compounds, suggesting that these molecules are more challenging to be converted than light ones.



RESEARCH ARTICLE

Figure 2. FPD+ signal for the hydrotreated oils over different catalysts. thiophene (T), benzothiophene (BT), dibenzothiophene (DBT), and 4,6-dimethyldibenzothiophene were used as standard. A linear fitting and their extrapolation correlating the sulfur compounds' retention time and their boiling point were plotted.

The ^{13}C -NMR functional group distribution in the HTL and HDT oils is reported in Figure 3. Both oils showed mainly an aliphatic fraction. However, we observed a considerable amount of unsaturated hydrocarbon components (aromatics, olefins) and carbonyl/carboxyl and ether/alcoholic components in the HTL oil. During the upgrading stage, the carbonyl compounds (e.g., carboxylic acids, esters, and fatty amides), alcohols, and ethers were converted and not detected by NMR analysis. The amount of olefinic and aromatic carbon decreased for the three HDT oils, which was more significant with the NiW sulfide catalyst than with the Ni phosphide and NiMo nitride catalysts. These results agree with the H/C ratio presented in Van Krevelen's diagrams (Figure 1), which shows that the sulfide catalyst has higher hydrogenation activity, contributing to a lower aromaticity degree.

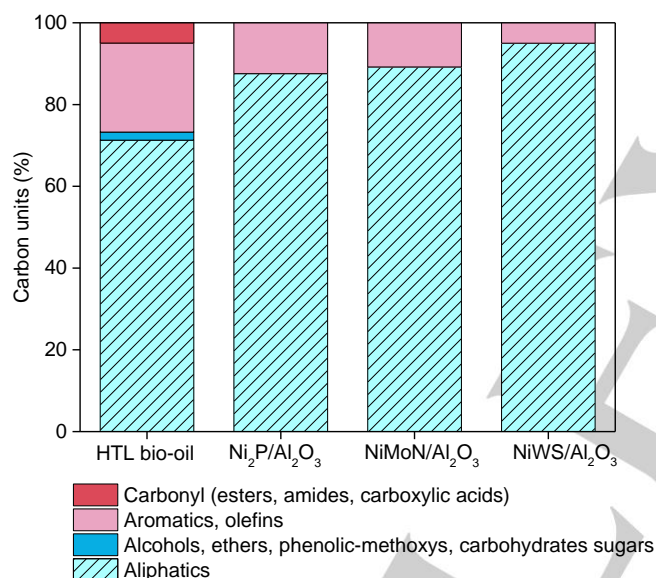


Figure 3. ^{13}C -NMR distribution by types of carbons in HTL and HDT oils over different catalysts.

Gel permeation chromatography coupled with a refractive index detector (GPC-RID) was employed to estimate the molecular weight of the HTL and HDT oils (Figure 4). The algal HTL oil showed the main intensity of around 300 g/mol, which can be associated with carboxylic acids (e.g., palmitic and stearic acids) in high amounts in algal oils.^[46] Moreover, heavy compounds with molecular weight above 400 g/mol are also present, in agreement with the literature.^[47] During the upgrading step, the main peak in the algal HTL oil was shifted to the left, which can be attributed to the conversion of fatty acids to aliphatics by decarboxylation/hydrogenation. Table 2 shows the average molecular weight of the HTL and HDT oils after treatment with and without a catalyst. On the one hand, HDT oil treated over $\text{Ni}_2\text{P}/\text{Al}_2\text{O}_3$ showed a molecular weight close to that of the HDT oil

treated without a catalyst. On the other hand, the NiMo nitride catalyst produced an HDT oil with higher molecular weight, suggesting that condensation reactions occurred when this catalyst was employed. Lastly, the NiW sulfide catalyst produced an HDT oil with a lower average molar mass, as can be observed by comparing the HDT oil elugrams in Figure 4 and reported in Table 2, indicating that heavy molecules were partially converted, which is in agreement with literature reports on the FT-ICR-MS analysis of HDT oils processed over sulfide catalysts^[48].

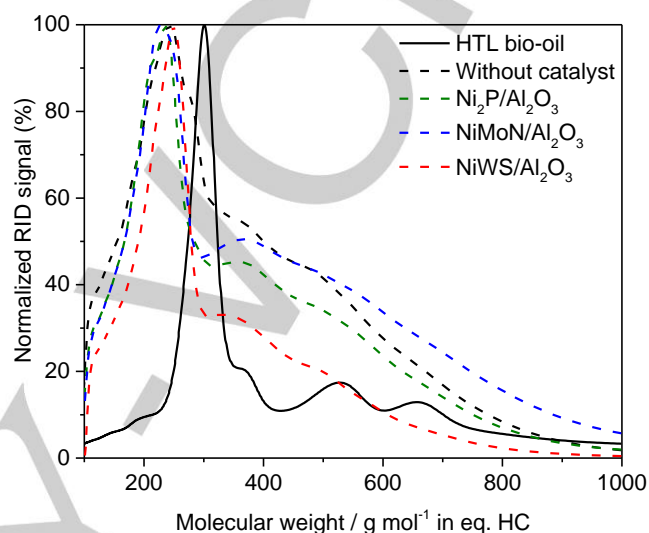


Figure 4. GPC-RID analysis of HTL and HDT oils over different catalysts.

Table 2. Average molecular weight for HTL and HDT oils with and without catalysts.

Sample	Average molecular mass Mw (g/mol in HC eq.)
HTL bio-oil	363
Without catalyst	287
$\text{Ni}_2\text{P}/\text{Al}_2\text{O}_3$	286
$\text{NiMoN}/\text{Al}_2\text{O}_3$	333
$\text{NiWS}/\text{Al}_2\text{O}_3$	264

Comprehensive two-dimensional gas chromatography coupled with a flame ionization detector and mass spectroscopy (GC \times GC-FID/MS) was employed to qualify and quantify the semi-volatile organic fraction of the HTL and HDT oils. Figure 5 shows the chromatogram obtained from the HDT oil processed over the Ni phosphide catalyst. Compared to the analysis of the HTL oil that shows mainly fatty acids, amides, and unsaturated (Figure S4), the main fraction was composed of aliphatic hydrocarbons, as corroborated by the ^{13}C -NMR analysis and reported by Rathack *et al.*^[49] A family of mono-aromatics was also identified in all chromatograms. High concentrations of C16 and C18 fatty nitriles and lighter nitriles were found in the HDT oil, processed over Ni_2P and without a catalyst. During the HTL reaction, fatty acids from

RESEARCH ARTICLE

the hydrolysis of the triglycerides can react with ammonia and amines through condensation reactions, forming fatty amides. Some works have reported the presence of these compounds in the algal HTL oil and mentioned that their concentration could be affected by the algae's biochemical composition.^[46,47] The 2D and 3D GCxGC chromatograms of the algal HTL oil (Figure S2) showed the presence of fatty amides, mainly composed of C16 and C18 chains. Zhu *et al.*^[50] recently reported that the hydroconversion of tertiary and secondary amides over NiMo/Al₂O₃ sulfide catalyst occurs via two pathways: deoxygenation followed by denitrogenation of the intermediate amine (main route) and denitrogenation followed by deoxygenation of the alkanol intermediate. Primary fatty amides should react similarly. However, with this kind of amide, it could be expected that the dehydration reaction could lead to fatty nitrile formation.^[51] Based on this, it is suggested that the C16 and C18 fatty nitriles reported in Figure 5 were formed from the dehydration of the fatty amides. This reaction also occurred without a catalyst. These nitriles were almost totally converted when NiW sulfide and NiMo nitride catalysts were employed. However, as mentioned before, both chromatograms obtained from the HDT oils treated over Ni₂P/Al₂O₃ and without catalyst showed a high amount of nitriles, mainly C16 and C18. Besides, a similar result was found when the Ni₂P/SiO₂ catalyst was employed, indicating that the Ni phosphide catalysts were less efficient for converting these compounds. Similar results were reported by Pongsiriyakul *et al.*^[52], who compared Ni-based catalysts promoted with Cu and Re supported on alumina. They found an HDT oil with high nitrogen content when Ni-Re/γ-Al₂O₃ was employed, which showed mainly nitrile compounds such as hexadecane nitrile. The quantification of the cyclic nitrogen compounds (e. g., indoles and carbazoles) and oxygen compounds (e.g., phenols) obtained with the GCxGC-FID/MS agreed with the oxygen and nitrogen content reported by the elemental analysis and the H/C ratio of the HDT oils. Therefore, NiWS/Al₂O₃ catalyst led to a liquid with a lower concentration of these compounds. As reported in the literature, a catalyst with higher hydrogenation activity favors the conversion of these molecules once the C-heteroatomic bond can be easily broken in a fully hydrogenated cyclic compound.^[53,54] In summary, GCxCG chromatograms of the HDT oils revealed that the Ni phosphide catalyst was less active in converting fatty nitriles and cyclic nitrogen compounds. In contrast, the NiWS catalyst resulted in an HDT oil with lower heteroatomic compounds due to a higher hydrogenation activity.

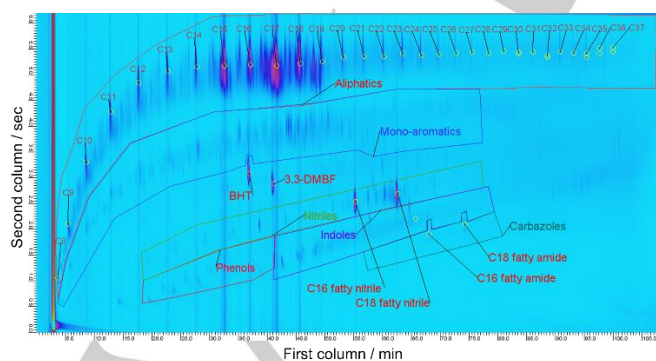


Figure 5. Comprehensive GCxGC-FID/MS chromatogram of HDT-oil over Ni₂P/Al₂O₃ catalyst.

As reported before, the C16 and C18 carboxylic acids were found in high amounts in the HTL oil and were easily converted during the upgrading stage. The first pathway is the decarboxylation/decarbonylation (DCO), leading to the formation of C15 and C17 n-alkanes in the liquid phase, implying the loss of one carbon by eliminating CO or CO₂ in the gas phase. The second pathway is hydrodeoxygenation (HDO), which preserves the number of carbon leading to C16 and C18 n-alkanes by removing water with higher hydrogen consumption.^[55,56] Based on this, the C16/C15 and C18/17 n-alkanes mass fraction ratios obtained with the GCxGC-FID were compared for the catalysts to illustrate the pathways taken for fatty acids conversion (Figure 6).

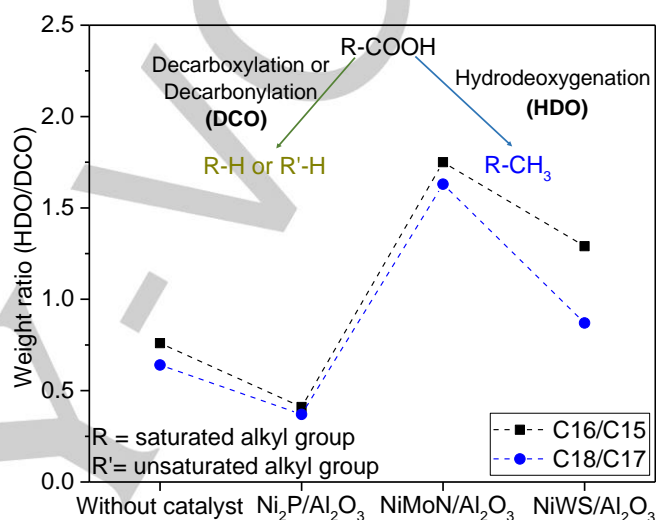


Figure 6. Hydrodeoxygenation and decarboxylation or decarbonylation ratio in function of catalyst.

Without a catalyst, the HDO/DCO ratio was lower than 1. It was even lower when the Ni phosphide catalyst was employed, indicating that DCO is favored without a catalyst and with Ni₂P. These results agree with Zarchin *et al.*^[57], who performed the hydroprocessing of soybean oil over a Ni phosphide catalyst supported on silica. They reported a C17 yield two times higher than C18. Besides, a similar trend was observed when Ni₂P/SiO₂ was employed and specific Ni sites favoring DCO pathway were proposed.^[58] It can be an advantage due to the lower H₂ consumption.^[59]

On the contrary, the NiMo nitride catalyst drastically promoted the HDO pathway compared to DCO. Similarly, Monnier *et al.*^[60] reported a molar ratio of n-C17/(n-C17 + n-C18) equal to 0.24 when Mo₂N/Al₂O₃ was employed in the hydroconversion of oleic acid, indicating that this catalyst favored the HDO route three times out of four DCO. Besides, the NiW sulfide catalyst showed an intermediate behavior compared to the Ni phosphide and NiMo nitride catalysts, with the two pathways being approximately equal. The simulated distillation profiles of HTL and HTD oils are shown in Figure 7, and the fractional cuts are in Table 3, respectively. The HTL oil curve shows two steps around 350 °C that can be associated with the C16 and C18 carboxylic acids. Note that the interaction of carboxylic acids with the column is different compared to n-alkanes, which results in a false boiling point. The boiling point of palmitic acid is 351 °C, and stearic acid is 361 °C.

RESEARCH ARTICLE

Using an FID detector, the response factor for carboxylic acids is approximately two times lower than the n-alkane utilized to calibrate the instrument. However, this analysis could also be used to corroborate the results found with GC×GC-FID/MS and GPC analysis, which showed the presence of these compounds. As expected, diesel was the main fraction obtained in the HDT oils due to the high concentration of C15-C18 aliphatics formed from the deoxygenation of the carboxylic acids.^[61] The NiMoN/Al₂O₃ catalyst resulted in a lower diesel fraction, probably due to condensation reactions, as mentioned before, since this HDT oil also showed a higher average molar mass than the others. Besides, the diesel fraction amount obtained from the Ni₂P/Al₂O₃ catalyst and without a catalyst should be considered carefully, since the C16 and C18 nitriles, which are still presented in these HDT oils, can elute in the diesel range, evidencing the importance of employing different techniques for the analyses of complex feeds.

Lastly, a heavy fraction composed of heavy gas oil and residual was found in all cases, with a lower amount when NiWS/Al₂O₃ was employed. As shown by the GPC analysis, the HTL algal bio-oil and hydrotreated oils are also composed of a heavy fraction that does not elute in the SIMDIS, resulting in a recovered mass close to 80 wt.% for hydrotreated oils. These results suggest that applying these operating conditions, a second stage must be used to convert these heavy compounds and increase the light fraction (jet fuel) that could produce sustainable aviation fuel (SAF).

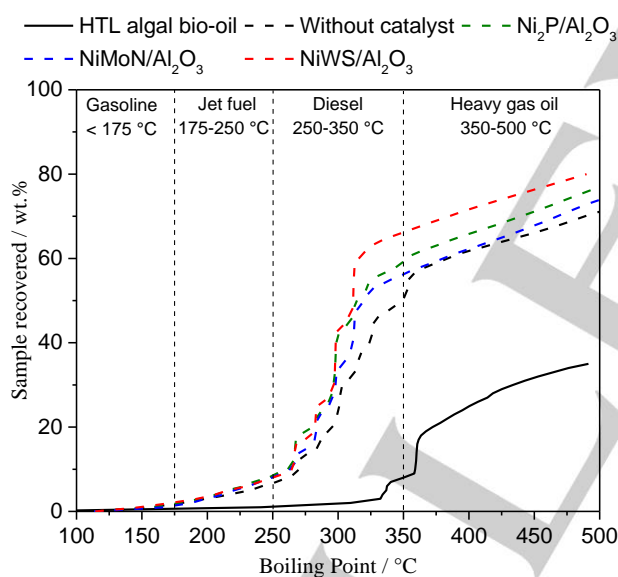


Figure 7. Simulated distillation profiles of HTL and HDT oils.

Table 3. Fractional cuts obtained from the simulated distillation of HTL and HDT oils (wt.%).

Sample	Gasoline	Jet fuel	Diesel	Heavy gas oil	Residual
HTL bio-oil	0	1	7	27	65
Without catalyst	1	5	44	21	29
NiMoN/Al ₂ O ₃	1	7	48	18	26

Ni ₂ P/Al ₂ O ₃	1	7	51	18	23
NiWS/Al ₂ O ₃	1	7	58	14	20

Conclusion

Several catalysts (Ni phosphide, NiMo nitride, and Ni (Mo, W) sulfides) were tested for the hydroconversion of algal bio-oil obtained from a continuous hydrothermal liquefaction reaction. The initial HTL algal oil was fully characterized, and C16-C18 fatty acids were identified as the main components but many kinds of nitrogen compounds are also present. The hydrotreated oils from experiments with catalysts showed lower oxygen and nitrogen content and higher HHV than that conducted without a catalyst. In summary, NiW sulfide catalysts performed better than NiMo nitride and Ni phosphide, showing a higher HHV, a lower aromaticity degree, and a lower average molar mass, indicating a better conversion of lipids. The Ni₂P/Al₂O₃ was more active than Ni₂P/SiO₂ for the hydroconversion of algal oil, suggesting that the support can highly affect the catalyst activity in this reaction. Besides, both catalysts promoted decarboxylation or decarbonylation reactions and were less active in converting fatty nitriles formed from the dehydration of fatty amides, indicating poor hydrogenation activity. On the contrary, the NiMoN/Al₂O₃ promoted the hydrodeoxygenation route and was more efficient than phosphide catalysts in converting fatty amides, as shown by GC×GC-FID/MS.

The NiWS/Al₂O₃ was the most active catalyst, showing a higher hydrogenation performance, evidenced by the H/C ratio, which resulted in the hydroconversion of refractory cyclic nitrogen compounds. In contrast, the NiWS/Silica-Al₂O₃ was the less active sulfide catalyst, probably due to the inhibition/deactivation due to the nitrogen compounds in high amounts of algal oil.

Therefore, sulfided catalysts, commonly used in refineries nowadays, showed promising results in the hydroconversion of algal bio-oil. Future research should focus on the stability of these catalysts at different times on stream using continuous reactors, since the presence of metal in the algal HTL oil, as well as the coke formation can affect the catalyst activity. In addition, hydrocracking of the partially hydrotreated fraction, composed mainly of diesel, to increase the production of a lighter fraction such as sustainable aviation fuel (SAF), can also be explored.

Experimental Section

Microalgae and HTL bio-oil production

Chlorella vulgaris NIES 227 (NIES-Collection, Japan) was grown in a photobioreactor in a greenhouse at MicroAlgae Processes Platform, CEA Cadarache, France. More details about microalgae cultivation were reported by Chambonniere *et al.*^[62]. The microalgae elemental and biochemical composition are reported in the supplementary material, Table S4. The HTL reaction of microalgae was performed in the continuous pilot-scale setup described elsewhere by CEA.^[63] The microalga was dispersed at 10 % of organic matter in water and injected into the reactor through a dual-syringe pump with a flow rate of 1.5 L/h so that the estimated residence time is in the order of 15 min. The pressure was set to 130 bar and the temperature to 300 °C. Then, bio-oil was extracted with dichloromethane.

Catalysts

Phosphide catalysts

Two phosphide catalysts supported on γ -Al₂O₃ (i) or SiO₂ (ii) were prepared. The nominal loading of the catalysts was 25 wt.% for Ni₂P/Al₂O₃ and Ni₂P/SiO₂. Before the catalyst preparation, both supports were calcinated at 500 °C for 3 h under airflow and dried at 120 °C for 1 h.

(i) The phosphide catalyst supported on sieved γ -Al₂O₃ (80 – 125 μ m) was prepared following the methodology reported by d'Aquino *et al.*^[33]. A stoichiometric amount of hypophosphorous acid (H₃PO₄, Sigma-Aldrich, 50 wt.% in H₂O) was added to nickel hydroxide (Ni(OH)₂, Sigma-Aldrich) to obtain a P/Ni atomic ratio equal to 2. Distilled water was added, and the solution was kept at 70 °C with stirring to ensure the total solid dissolution. Then, the green light solution was impregnated onto the support until incipient wetness. Several impregnations were necessary, and the catalyst was dried at 70 °C between them for approximately 1 h. After the last impregnation, the catalyst was dried for 24 h at 70 °C. Following the drying, two reduction steps were performed: the first followed by passivation for catalyst characterization and the second without passivation to measure the catalyst activity during the upgrading step. Approximately 0.7g of the catalyst precursor was transferred to a quartz U-tube and degassed in 50 mL/min N₂ for 30 min. Afterward, the precursor was subjected to TPR in H₂ flowed at 50 mL/min by heating from room temperature to 500 °C (heating rate of 5 °C/min) after holding for 1 h. The Ni₂P/Al₂O₃ was cooled to room temperature in continued H₂ flow. When a passivation step was performed, the catalyst was purged with N₂ for 30 min following passivation with a mixture of 50 mL/min N₂ and 10 mL/min air for 2 h.

(ii) The phosphide catalyst supported on SiO₂ was prepared following the methodology reported by Bowker *et al.*^[29]. A stoichiometric amount of ammonium dihydrogen phosphate (NH₄H₂PO₄, Alfa Aesar, 98%) and nickel nitrate hexahydrate (Ni(NO₃)₂·6H₂O, Alfa Aesar, 98%) was added to a beaker to obtain a P/Ni atomic ratio equal to 0.9. Sufficient distilled water was added under constant stirring, and the pH of the impregnation solution was adjusted to nitric acid (HNO₃, Honeywell Fluka™, \geq 65%) until complete solubilization of the precipitate. The resulting impregnation solution was used for the impregnation of the support by the incipient wetness impregnation method. Several impregnations were necessary, and the catalyst was dried between them at 120 °C for approximately 1 h. After the last impregnation, the precursor was dried for 24 h at 120 °C and then calcinated for 3 h at 500 °C (heating rate of 10 °C/min) under air. Following the calcination, two reduction steps were performed: the first followed by passivation for catalyst characterization and the second without passivation to measure the catalyst activity during the upgrading step. Approximately 0.7 g of the catalyst precursor was transferred to a quartz U-tube and degassed in 50 mL/min N₂ for 30 min. Afterward, the precursor was subjected to TPR in H₂ and flowed at 50 mL/min by heating from room temperature to 650 °C (heating rate of 1 °C/min) after holding for 2 h. The Ni₂P/SiO₂ was cooled to room temperature in continued H₂ flow. When a passivation step was performed, the catalyst was purged with N₂ for 30 min following passivation with a mixture of 50 mL/min N₂ and 10 mL/min air for 2 h.

Nitride catalysts

Two NiMo nitride catalysts were prepared following the methodology reported by Chouzier *et al.*^[37,38]: a bulk catalyst, named NiMoN, and another supported on γ -Al₂O₃, named NiMoN/Al₂O₃. Aqueous solutions of ammonium heptamolybdate ((NH₄)₆Mo₇O₂₄·4H₂O, Sigma-Aldrich, 99%), nickel nitrate hexahydrate (Ni(NO₃)₂·6H₂O, Alfa Aesar, 98%) and hexamethylenetetramine (HMTA) (N₄(CH₂)₆, Sigma-Aldrich, 98%) were mixed under stirring. The atomic ratio Ni/Mo was 0.5; the atomic ratio of carbon from HMTA to the sum of metals C/(Ni+Mo) was 32. The formed precipitate was washed with distilled water and dried under nitrogen flow at 200 °C overnight. Then, the catalyst precursor was placed in a quartz reactor and heated for 2 h at 650 °C (heating rate of 10 °C/min) under N₂.

The NiMoN/Al₂O₃ showed a nominal loading of 16.7 wt% MO₃ and 6.7 wt.% NiO.

Sulfide catalysts

A commercial NiW/Al₂O₃ extrudate catalyst^[64] (WO₃: 25.7 wt.%, NiO: 3.8 wt.%) was used as a reference, and two catalysts with CA/Ni molar ratio equal to 2 and the same metal content as the reference catalyst were prepared using post-treatment (i) and co-impregnation (ii) as preparation methods.

(i) Sufficient citric acid (C₆H₈O₇·H₂O, Sigma-Aldrich, 99%) was added to distilled water with stirring. This solution was used to impregnate the NiW/Al₂O₃ catalyst, previously dried at 120 °C for 1 h, until incipient wetness. Then, the catalyst aged for 12 h at room temperature and dried at 120 °C for 12 h. This catalyst was named NiW/Al₂O₃ + CA.

(ii) Ammonium metatungstate hydrate ((NH₄)₆W₁₂O₄₀·xH₂O, Sigma-Aldrich, \geq 66.5%) was dissolved in distilled water, and this solution was used to impregnate an extrudate γ -Al₂O₃, previously calcinated at 500 °C for 3 h under airflow and dried at 120 °C for 1 h. Then, the tungsten-alumina base catalyst was aged for 12 h at room temperature and dried at 120 °C for 12 h. Afterward, nickel nitrate hexahydrate (Ni(NO₃)₂·6H₂O, Alfa Aesar, 98%) was dissolved in distilled water, and citric acid was added. The pH of the solution was adjusted to 5 by adding ammonium hydroxide (NH₄OH, Honeywell Fluka™, 30-33 % NH₃ in H₂O) to optimize the formation of active NiWS species.^[65] Then, the resulting solution was used to impregnate the tungsten-alumina base catalyst until incipient wetness. The resulting catalyst was aged for 12 h at room temperature and dried at 120 °C for 12 h. This catalyst was named NiW(CA)/Al₂O₃.

Moreover, two other catalysts were tested: NiW/silica-alumina (WO₃: 26.5 wt.%, NiO: 3.8 wt.%, SiO₂: 19.3 wt.%) and NiMo(P)/Al₂O₃ (MoO₃: 18.6 wt.%, NiO: 3.8 wt.%, P₂O₅: 4.9 wt.%).

Before characterization and catalytic activity experiments, the catalysts were sulfided *ex situ* at 400 °C (heating rate of 5 °C/min) for 3 h under 15% H₂S/H₂ flow (4 NL/h) except the NiW(CA)/Al₂O₃ which was sulfided at 400 °C (heating rate of 3 °C/min) for 2 h under 15% H₂S/H₂ flow (4 NL/h).

Catalytic hydrotreatment of HTL algal bio-oil

The upgrading step was performed using a 300 mL Parr stainless steel batch reactor. Firstly, 0.6 g *ex situ* activated catalyst, 3.0 g of HTL bio-oil, and 25 g of n-heptane were added to the reactor. Subsequently, the reactor was closed, purged with N₂, and 6 MPa was loaded for a leak test. Then, the N₂ was removed, and the reactor was purged three times with H₂, loaded with 1 MPa of H₂, and heated to 375 °C. Once the temperature had been reached, 5 MPa of H₂ was added to get a total pressure of 10 MPa, and the stirring at approximately 570 rpm was started. The reaction was performed for 5 h, and the system was cooled. The used catalyst was separated from the hydrotreated oil (HDT-oil) by filtration, and n-heptane was used to wash the reactor to recover the residual catalyst and oil. The n-heptane was further removed using a vacuum evaporator, and different analytical techniques were used to analyze the HDT oil.

Characterization of analytic techniques

The C, H, O, N, and S mass fractions were analyzed in a Thermo Scientific Flash 2000 Apparatus. ANTEK 9000NS was used for S analyses, which is more precise (from low ppb until percent levels) and accurate. The HTL bio-oil and HDT-oil were diluted using THF to a concentration of 5 wt.% and 10 wt.%, respectively, then injected into a reactor at 1050 °C. The higher heating value (HHV) was calculated based on elemental analysis values according to the equation reported by Channiwala and Parikh.^[66]

An Agilent 7890A GC coupled with an FPD+ detector and fitted with a GC column (HP-5: 30 m x 0.32 mm x 0.25 µm) was employed to analyze the sulfur compounds. In addition, thiophene (C₄H₄S, Sigma-Aldrich, >99%), benzothiophene (C₈H₆S, Sigma-Aldrich, 98%), dibenzothiophene (C₁₂H₈S, Acros Organics, 95%), and 4,6-dimethyldibenzothiophene (C₁₄H₁₂S, Janssen Chimica, 95%) were injected to provide some insights regarding the sulfur compounds in the algal oil.

The gel permeation analyses were performed using an Agilent 1200 series HPLC equipped with two PLgel Columns (50 and 500 Å) and a differential refractive index detector (RID). The analyses were carried out at 35 °C using THF as eluent with a 1 mL/min flow rate. Before analyses, the samples were diluted to a concentration of approximately 1 wt.% in THF and filtered (0.45 µm). The elution time was converted into molecular weight (Mw) using a calibration curve obtained with a hydrocarbon mixture (Mw from 86 to 1000 g/mol). The elugrams obtained from the RID detector were normalized to the highest peak intensity.

¹³C-NMR spectra were recorded with a Bruker AVANCE 400 MHz spectrometer and analyzed using the software TopSpin 3.0. The measurements were performed at room temperature with an accumulation of 4700 scans for approximately 15 h. The samples (60 mg) were diluted with deuterated chloroform (CDCl₃).

The boiling point distributions were determined utilizing simulated distillation (SimDis) according to the standard ASTM D2887. The analyses were performed on an Agilent 7890A GC coupled with an FID and fitted with a GC column (CP-SimDist UltiMetal: 10 m x 0.53 mm x 2.65 µm). The liquid products were defined by five boiling point ranges: gasoline (< 175 °C), jet fuel (175–250 °C), diesel (250–350 °C), heavy gas oil (350–500 °C), and residual (> 500 °C).

The GC×GC analysis was performed using two systems: The first one was a GC Agilent 6890 with a cryogenic modulator from Zoex Corporation (USA) connected to a mass spectrometer (MS) 5975B for the identification of compounds (up to C32) and fitted with two columns (VF-1701-MS: 30 m x 0.25 mm x 0.25 µm and DB-1: 3 m x 0.1 mm x 0.1 µm). The second one was a GC Agilent 7890A with a flow modulator connected to an FID for quantification (up to C40) and fitted with two columns (ZB-1701: 15 m x 0.10 mm x 0.05 µm and DB-1: 5 m x 0.25 mm x 0.25 µm). Modulation parameters were optimized according to Lelevic *et al.*^[67]. The samples were diluted in THF to a concentration of around 10 wt.% and 5 wt.% for MS and FID analysis, respectively. Besides, an internal standard, 3,3'-dimethylbiphenyl (C₁₄H₁₄, Sigma-Aldrich, 99%), 200 mg/kg, was also added for quantification purposes.

Acknowledgments

This project has received funding from ANR for the project RAFBIOALG 18-CE43-009. Bruno da Costa Magalhães thanks the ANR for providing a Ph.D. grant.

The authors thank CEA Cadarache and CEA Grenoble for providing the microalgae and the HTL bio-oil, respectively.

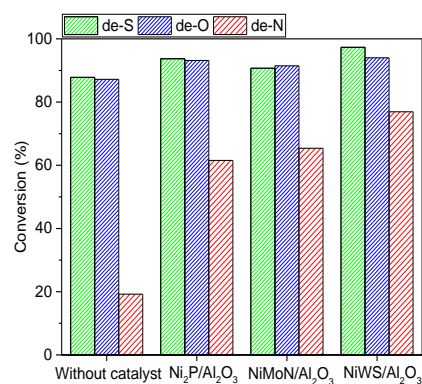
Keywords: • biofuel • biomass • heterogeneous catalysis • hydrothermal liquefaction • hydrotreatment

- [1] A. Ramirez-Romero, B. Da Costa Magalhães, A. Dimitriades-Lemaire, J. F. Sassi, F. Delrue, J. P. Steyer, *Fermentation* **2022**, *8*, 1–15.
 [2] L. Garcia Alba, C. Torri, C. Samori, J. Van Der Spek, D. Fabbri, S. R. A. Kersten, D. W. F. Brilman, *Energy and Fuels* **2012**, *26*, 642–657.
 [3] S. Martinez-Villarreal, A. Breitenstein, P. Nimmegeers, P. Perez Saura, B. Hai, J. Asomaning, A. A. Eslami, P. Billen, S. Van Passel, D. C. Bressler, D. P. Debecker, C. Remacle, A. Richel, *Biomass and Bioenergy* **2022**, *165*, 106555.

- [4] J. Yu, M. Audu, M. T. Myint, F. Cheng, J. M. Jarvis, U. Jena, N. Nirmalakhandan, C. E. Brewer, H. Luo, *Fuel Process. Technol.* **2022**, *227*, 107119.
 [5] S. K. Ratha, N. Renuka, T. Abunama, I. Rawat, F. Bux, *Renew. Sustain. Energy Rev.* **2022**, *156*, 111973.
 [6] D. M. Santosa, L. M. Wendt, B. D. Wahlen, A. J. Schmidt, J. Billing, I. V. Kutnyakov, R. T. Hallen, M. R. Thorson, T. L. Oxford, D. B. Anderson, *Algal Res.* **2022**, *62*, 102622.
 [7] P. Biller, A. B. Ross, *Bioresour. Technol.* **2011**, *102*, 215–225.
 [8] H. Li, Z. Liu, Y. Zhang, B. Li, H. Lu, N. Duan, M. Liu, Z. Zhu, B. Si, *Bioresour. Technol.* **2014**, *154*, 322–329.
 [9] M. S. Haider, D. Castello, L. A. Rosendahl, *Energy and Fuels* **2021**, *35*, 10611–10622.
 [10] J. M. Jarvis, N. M. Sudasinghe, K. O. Albrecht, A. J. Schmidt, R. T. Hallen, D. B. Anderson, J. M. Billing, T. M. Schaub, *Fuel* **2016**, *182*, 411–418.
 [11] M. Salman, S. Chiaberge, A. Siviero, M. Akif, D. Castello, T. Helmer, L. Aistrup, *Fuel* **2023**, *334*, 126755.
 [12] S. Leow, J. R. Witter, D. R. Vardon, B. K. Sharma, J. S. Guest, T. J. Strathmann, *Green Chem.* **2015**, *17*, 3584–3599.
 [13] C. Yang, R. Li, C. Cui, S. Liu, Q. Qiu, Y. Ding, Y. Wu, B. Zhang, *Green Chem.* **2016**, *18*, 3684–3699.
 [14] G. W. Huber, A. Corma, *Angew. Chemie - Int. Ed.* **2007**, *46*, 7184–7201.
 [15] D. C. Elliott, T. R. Hart, A. J. Schmidt, G. G. Neuenschwander, L. J. Rotness, M. V. Olarte, A. H. Zacher, K. O. Albrecht, R. T. Hallen, J. E. Holladay, *Algal Res.* **2013**, *2*, 445–454.
 [16] K. O. Albrecht, Y. Zhu, A. J. Schmidt, J. M. Billing, T. R. Hart, S. B. Jones, G. Maupin, R. Hallen, T. Ahrens, D. Anderson, *Algal Res.* **2016**, *14*, 17–27.
 [17] B. Zhao, Z. Shi, X. Yang, *Ind. Eng. Chem. Res.* **2017**, *56*, 6378–6390.
 [18] J. M. Jarvis, K. O. Albrecht, J. M. Billing, A. J. Schmidt, R. T. Hallen, T. M. Schaub, *Energy and Fuels* **2018**, *32*, 8483–8493.
 [19] M. S. Haider, D. Castello, L. A. Rosendahl, *Biomass and Bioenergy* **2020**, *139*, 105658.
 [20] A. Stanislaus, A. Marafi, M. S. Rana, *Catal. Today* **2010**, *153*, 1–68.
 [21] M. D. Mello, F. A. Braggio, B. C. Magalhães, J. L. Zotin, M. A. P. Silva, *Ind. Eng. Chem. Res.* **2017**, *56*, 10287–10299.
 [22] T. Zhou, H. Yin, S. Han, Y. Chai, Y. Liu, C. Liu, *J. Fuel Chem. Technol.* **2009**, *37*, 330–334.
 [23] F. A. Braggio, M. Dorneles De Mello, B. C. Magalhães, J. L. Zotin, M. A. P. Silva, *Energy and Fuels* **2019**, *33*, 1450–1457.
 [24] L. Oliviero, F. Maugé, P. Afanasiev, C. Pedraza-Parra, C. Geantet, *Catal. Today* **2021**, *377*, 3–16.
 [25] P. Biller, B. K. Sharma, B. Kunwar, A. B. Ross, *Fuel* **2015**, *159*, 197–205.
 [26] B. Guo, V. Walter, U. Hornung, N. Dahmen, *Fuel Process. Technol.* **2019**, *191*, 168–180.
 [27] X. Liu, Y. Guo, A. Dasgupta, H. He, D. Xu, Q. Guan, *Renew. Energy* **2022**, *183*, 627–650.
 [28] A. Galadima, A. Masudi, O. Muraza, *Mol. Catal.* **2022**, *523*, 112131.
 [29] R. H. Bowker, B. Ilic, B. A. Carrillo, M. A. Reynolds, B. D. Murray, M. E. Bussell, *Appl. Catal. A Gen.* **2014**, *482*, 221–230.
 [30] A. Cole, Y. Dinburg, B. S. Haynes, Y. He, M. Herskowitz, C. Jazrawi, M. Landau, X. Liang, M. Magnusson, T. Maschmeyer, A. F. Masters, N. Meiri, N. Neveux, R. De Nys, N. Paul, M. Rabaev, R. Vidruk-Nehemya, A. K. L. Yuen, *Energy Environ. Sci.* **2016**, *9*, 1828–1840.
 [31] S. T. Oyama, T. Gott, H. Zhao, Y. K. Lee, *Catal. Today* **2009**, *143*, 94–107.
 [32] M. E. Bussell, *React. Chem. Eng.* **2017**, *2*, 628–635.
 [33] A. I. D'Aquino, S. J. Danforth, T. R. Clinkingbeard, B. Ilic, L. Pullan, M. A. Reynolds, B. D. Murray, M. E. Bussell, *J. Catal.* **2016**, *335*, 204–214.
 [34] D. J. Sajkowski, S. T. Oyama, *Appl. Catal. A Gen.* **1996**, *134*, 339–349.
 [35] Y. Chu, Z. Wei, S. Yang, C. Li, Q. Xin, E. Min, *Appl. Catal. A-general* **1999**, *176*, 17–26.
 [36] W. Yuhong, L. Wei, Z. Minghui, G. Naijia, T. Keyi, *Appl. Catal. A Gen.* **2001**, *215*, 39–45.
 [37] S. Chouzier, P. Afanasiev, M. Vrinat, T. Cseri, M. Roy-Auberger, *J. Solid State Chem.* **2006**, *179*, 3314–3323.
 [38] S. Chouzier, M. Vrinat, T. Cseri, M. Roy-Auberger, P. Afanasiev, *Appl. Catal. A Gen.* **2011**, *400*, 82–90.
 [39] K. Ramasamy, M. R. Thorson, J. M. Billing, J. E. Holladay, C. Drennan, B. Hoffman, Z. Haq, **2021**, Hydrothermal Liquefaction: Path to Sustainable Aviation Fuel. United States: N. p., DOI:10.2172/1821809.
 [40] R. W. Gosselink, S. A. W. Hollak, S. W. Chang, J. Van Haveren, K. P. De Jong, J. H. Bitter, D. S. Van Es, *ChemSusChem* **2013**, *6*, 1576–1594.
 [41] M. T. Nguyen, G. D. Pirngruber, F. Albriex, F. Chainet, M. Tayakout-Fayolle, C. Geantet, *Energy and Fuels* **2019**, *33*, 1467–1472.
 [42] J. M. Jarvis, J. M. Billing, R. T. Hallen, A. J. Schmidt, T. M. Schaub, *Energy and Fuels* **2017**, *31*, 2896–2906.
 [43] M. S. Haider, D. Castello, L. A. Rosendahl, *Biomass and Bioenergy* **2020**, *139*, 105658.

- [44] A. A. Shah, K. Sharma, M. S. Haider, S. S. Toor, L. A. Rosendahl, T. H. Pedersen, D. Castello, *Processes* **2022**, *10*, 207.
- [45] D. Xu, G. Lin, S. Guo, S. Wang, Y. Guo, Z. Jing, *Renew. Sustain. Energy Rev.* **2018**, *97*, 103–118.
- [46] R. B. Madsen, H. Zhang, P. Biller, A. H. Goldstein, M. Glasius, *Energy and Fuels* **2017**, *31*, 4122–4134.
- [47] F. Cheng, Z. Cui, L. Chen, J. Jarvis, N. Paz, T. Schaub, N. Nirmalakhandan, C. E. Brewer, *Appl. Energy* **2017**, *206*, 278–292.
- [48] J. Zuber, H. Wollmerstädt, T. Kuchling, S. Kureti, P. Rathsack, *Energy & Fuels* **2020**, *34*, 3199–3209.
- [49] P. Rathsack, H. Wollmerstaedt, T. Kuchling, S. Kureti, *Fuel* **2019**, *248*, 178–188.
- [50] C. Zhu, O. Y. Gutiérrez, D. M. Santosa, M. Flake, R. Weindl, I. Kutnyakov, H. Shi, H. Wang, *Appl. Catal. B Environ.* **2022**, *307*, 121197.
- [51] M. A. R. Jamil, S. M. A. H. Siddiki, A. S. Touchy, M. N. Rashed, S. S. Poly, Y. Jing, K. W. Ting, T. Toyao, Z. Maeno, K. ichi Shimizu, *ChemSusChem* **2019**, *12*, 3115–3125.
- [52] K. Pongsiriyakul, W. Kiatkittipong, S. Adhikari, J. Wei, **2021**, 216.
- [53] V. N. Bui, D. Laurenti, P. Afanasiev, C. Geantet, *Appl. Catal. B Environ.* **2011**, *101*, 239–245.
- [54] M. T. Nguyen, G. D. Pirngruber, F. Chainet, M. Tayakout-Fayolle, C. Geantet, *Ind. Eng. Chem. Res.* **2017**, *56*, 11088–11099.
- [55] M. Ruinat De Brimont, C. Dupont, A. Daudin, C. Geantet, P. Raybaud, *J. Catal.* **2012**, *286*, 153–164.
- [56] M. Snåre, I. Kubičková, P. Mäki-Arvela, K. Eränen, D. Y. Murzin, *Ind. Eng. Chem. Res.* **2006**, *45*, 5708–5715.
- [57] R. Zarchin, M. Rabaev, R. Vidruk-Nehemya, M. V. Landau, M. Herskowitz, *Fuel* **2015**, *139*, 684–691.
- [58] D. A. Ruddy, J. A. Schaidle, J. R. Ferrell, J. Wang, L. Moens, J. E. Hensley, *Green Chem.* **2014**, *16*, 367–490.
- [59] M. de Oliveira Camargo, J. L. Castagnari Willimann Pimenta, M. de Oliveira Camargo, P. A. Arroyo, *Fuel* **2020**, *281*, 118719.
- [60] J. Monnier, H. Sulimma, A. Dalai, G. Caravaggio, *Appl. Catal. A Gen.* **2010**, *382*, 176–180.
- [61] D. Castello, M. S. Haider, L. A. Rosendahl, *Renew. Energy* **2019**, *141*, 420–430.
- [62] P. Chambonniere, A. Ram, F. Delrue, A. Dimitriades-lemaire, J. Sassi, *Fermentation* **2022**, *8*, 614.
- [63] C. Barrère-Mangote, A. Roubaud, B. Bouyssiere, J. Maillard, J. Hertzog, J. Le Maître, M. Hubert-Roux, J. F. Sassi, C. Afonso, P. Giusti, *Processes* **2021**, *9*, 1494.
- [64] C. Gachet, M. Breysse, M. Cattenot, T. Decamp, R. Frety, M. Lacroix, L. de Mourgues, J. L. Portefaix, M. Vrinat, J. C. Duchet, S. Housni, M. Lakhdar, M. J. Tilliette, J. Bachelier, D. Cornet, P. Engelhard, C. Gueguen, H. Toulhoat, *Catal. Today* **1988**, *4*, 7–22.
- [65] V. A. Suárez-Toriello, C. E. Santolalla-Vargas, J. A. De Los Reyes, A. Vázquez-Zavala, M. Vrinat, C. Geantet, *J. Mol. Catal. A Chem.* **2015**, *404–405*, 36–46.
- [66] S. A. Channiwala, P. P. Parikh, *Fuel* **2002**, *81*, 1051–1063.
- [67] A. Lelevic, V. Souchon, C. Geantet, C. Lorentz, M. Moreaud, *J. Chromatogr. A* **2020**, *1626*, 461342.

Entry for the Table of Contents



Supported metal phosphide, nitride, and sulfide catalysts were compared for the hydroconversion of algal oil. Nickel phosphide catalysts promoted the decarboxylation/decarbonylation route for the conversion of carboxylic acids, while NiMo nitride catalysts promoted the hydrodeoxygenation pathway. NiWS/Al₂O₃ sulfide was the best catalyst resulting in a hydrotreated oil with lower heteroatom content and average molar mass that fell primary in the diesel range.

Institute and/or researcher Twitter usernames: @ircelyon